

# DeepTrace: Learning to Optimize Contact Tracing in Epidemic Networks with Graph Neural Networks

Siya Chen, Pei-Duo Yu, Chee Wei Tan and H. Vincent Poor

**Abstract**—The goal of digital contact tracing is to diminish the spread of an epidemic or pandemic by detecting and mitigating public health emergencies using digital technologies. Since the start of the COVID-19 pandemic, a wide variety of mobile digital apps have been deployed to identify people exposed to the SARS-CoV-2 coronavirus and to stop onward transmission. Tracing sources of spreading (i.e., backward contact tracing), as has been used in Japan and Australia, has proven crucial as going backwards can pick up infections that might otherwise be missed at superspreading events. How should robust backward contact tracing automated by mobile computing and network analytics be designed? In this paper, we formulate the forward and backward contact tracing problem for epidemic source inference as maximum-likelihood (ML) estimation subject to subgraph sampling. Besides its restricted case (inspired by the seminal work of Zaman and Shah in 2011) when the full infection topology is known, the general problem is more challenging due to its sheer combinatorial complexity, problem scale and the fact that the full infection topology is rarely accurately known. We propose a Graph Neural Network (GNN) framework, named DeepTrace, to compute the ML estimator by leveraging the likelihood structure to configure the training set with topological features of smaller epidemic networks as training sets. We demonstrate that the performance of our GNN approach improves over prior heuristics in the literature and serves as a basis to design robust contact tracing analytics to combat pandemics.

**Index Terms**—Digital contact tracing, Epidemic source inference, Maximum likelihood estimation, Graph neural network

## I. INTRODUCTION

Since the start of the COVID-19 pandemic, a wide variety of mobile apps [1]–[4] have been deployed to identify people exposed to the SARS-CoV-2 coronavirus and to stop its onward transmission. These mobile apps provide exposure notifications that complement the traditional contact tracing, which can be labor-intensive and slow. Mobile computing and data analytics can potentially scale up to cover an entire population automatically, which is especially useful for tracking a fast-spreading disease and its variants. The goal of digital contact tracing is thus to diminish the spread of the epidemic, but this is complicated by factors such as the speed of disease

S. Chen is with the Department of Computer Science, City University of Hong Kong, Hong Kong (e-mail: siyachen4-c@my.cityu.edu.hk).

P. D. Yu is with the Department of Applied Mathematics, Chung Yuan Christian University, Taiwan (e-mail: peiduoyu@cycu.edu.tw).

C. W. Tan is with Nanyang Technological University, Singapore, Nanyang Ave., Singapore (e-mail: cheewei.tan@ntu.edu.sg).

H. V. Poor is with the Department of Electrical and Computer Engineering, Princeton University, Princeton, NJ 08544 USA (e-mail: poor@princeton.edu).

This work is supported in part by the U.S. National Science Foundation under RAPID Grant IIS-2026982, the Ministry of Science and Technology of Taiwan under Grant 110-2115-M-033-001-MY2, Hong Kong ITF Project ITS/188/20 and an Institute for Pure and Applied Mathematics fellowship.

spreading, asymptomatic infections and the presence of superspreaders whereby approximately 20% of infected individuals are responsible for 80% of transmissions. Designing robust contact tracing automated by mobile computing and network analytics is still in its infancy.

It has been recently shown in [2], [5]–[8] that, compared with ‘forward’ tracing (i.e., to whom disease spreads), ‘backward’ tracing (from whom disease spreads) can be more effective due to overlooked biases arising from the heterogeneity in contacts. Tracing sources of spreading (i.e., backward contact tracing), as had been used in Japan and Australia, has proven effective as going backwards can pick up infections that might otherwise be missed at superspreading events. The ability to identifying the source of spreading (i.e., the Patient Zero or superspreaders in a pandemic) is essential to contact tracing.

The epidemic source inference problem was first studied in the seminal work [9] as a maximum likelihood estimation problem based on a Susceptible-Infectious (SI) model [10], which is a special case of the classical susceptible-infected-recover (SIR) model in epidemiology [11]–[13]. This problem is invariably hard to solve due to the need to track the likelihood of permitted permutations of nodes in the graph (corresponding to the spreading instance over the given network) and to count the number of permitted permutations for each node in the graph. For the degree-regular tree special case, this problem can be solved in polynomial time by a network centrality approach, i.e., the *rumor centrality* in [9], [14]) is proportional to the number of permitted permutations. Equivalently, this optimal likelihood estimate is the graph centroid [15], [16]. The network centrality approach in [9] has been extended to scenarios like random trees [17], [18], multiple snapshot observations [19], and multiple sources [20]. Different from the snapshot model in [9], the authors in [21], [22] propose using noisy time-series data model and Bayesian analysis to solve the epidemic source inference problem by the sequential detection and quickest detection techniques.

In this paper, we formulate a backward contact tracing problem that leverages the aforementioned maximum likelihood estimation as a subproblem, and design contact tracing algorithms based on a network centrality design approach. However, computing the network centrality for a large graph can be computationally challenging. There are works using GNNs<sup>1</sup> to compute the eigenvector centrality [25] and the betweenness centrality [26]. Our paper describes how network centrality can be useful for solving a maximum likelihood estimation problem that underlies backward contact tracing. There

<sup>1</sup>An overview of GNNs can be found in [23], [24].

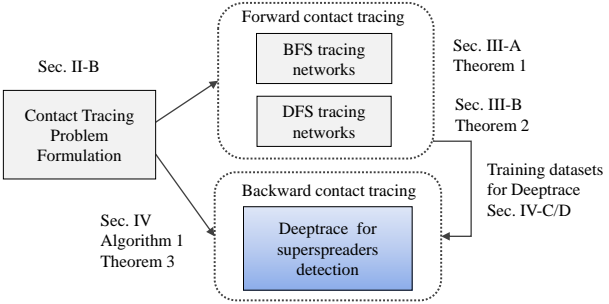


Fig. 1: The overview of DeepTrace algorithm for digital contact tracing in epidemic networks.

are also recent related works on GNNs for pandemic control in [27], [28]. The authors in [28] used graph convolutional networks that however can only be used in a "transductive" setting (i.e., the trained network model cannot be used for graph input of different sizes). Our work differs from these prior works in that we use an inductive version of GNN to regress the network centrality and to solve the maximum likelihood estimation problem for networks of different scales (which is more realistic to model the dynamical effects of the pandemic spreading over time). This also leads to a low-complexity digital contact tracing algorithm that can iteratively refine the most-likely epidemic source estimate.

The main contributions of this paper are:

- 1) We formulate a backward contact tracing problem as maximum-likelihood estimation that is then solved by a GNN framework using forward contact tracing with breadth-first search (BFS) and depth-first search (DFS) tracing strategy as well as backward contact tracing to search for superspreaders.
- 2) The novelty is to train the GNN using smaller graphs harvested by forward contact tracing and then to find the most-likely superspreader via backward contact tracing using computationally-efficient estimators for aggregating the spreading probabilities.
- 3) Using synthetic datasets and real-world contact tracing data in Hong Kong and Taiwan, we demonstrate that our algorithms outperform the state-of-the-art heuristic in [9].

The paper is organized as follows. We briefly review epidemic spreading models and formulate a contact tracing problem in Section II. We detail interesting insights into tracing superspreaders in contact tracing networks obtained using BFS and DFS tracing strategies for forward contact tracing in Section III. We propose a GNN learning framework for general graphs using low-complexity techniques for supervised learning in Section IV. We provide performance evaluation comparisons for synthetic and real-world contact tracing networks in Section V. Finally, Section VI concludes the paper.

## II. CONTACT TRACING PROBLEM FORMULATION

Let us first introduce the spreading models including one relevant to COVID-19 in [13] and then present the digital contact tracing optimization problem formulation followed by its mathematical analysis.

### A. Epidemic Spreading Model

There are numerous models in the study of the spread of infectious diseases ranging from well-known ones like the Susceptible-Infectious (SI) model to Susceptible-Infectious-Recovery-Susceptible (SIRS) models [12], [13]. Despite being the most basic one, we focus primarily on the SI model for analysis, since the SI model can model the pandemic in its early stage. Suppose the virus spreads over a network modeled by a graph  $G$  whose nodes and edges model persons and their social contacts, respectively. The virus starts from a node in  $G$  (i.e., the superspreader) and spreads to other nodes through their connection, yielding an epidemic network  $G_N$  at some point in time, where  $N$  represents the number of infected nodes in  $G_N$ . This epidemic network  $G_N$  and the infection spreading dynamics are assumed to be unknown to a contact tracer, who therefore adopts a strategy to collect this data starting from an index case (i.e., the first documented infected person) and trace his or her close contacts and so on.

### B. Backward Contact Tracing Problem

At various stages of contact tracing, we model an instantaneous snapshot of a subgraph of  $G_N$  that we call the *contact tracing network* being harvested. This contact tracing network grows by one (infected) node at each stage. If the traced node is infected, we continue to trace the node's neighbors, otherwise we stop tracing along this node. Let  $G_n$  denote the contact tracing network with  $n$  nodes at the  $n$ -th stage of tracing (the index case is  $G_1$ ). Obviously,  $G_n \subseteq G_N \subseteq G$ . A goal of contact tracing is to find the node in  $G_N$  that is most likely to be the superspreader, as shown in Fig. 2. However, the superspreader may not yet be in  $G_n$ , meaning that the contact tracing effort is still in its early stage or not fast enough (relative to the pandemic spreading speed). In such a case, backward contact tracing should yield an estimate as close as possible to this most-likely superspreader. In other words, given the available data at the  $n$ -th stage, the contact tracer finds the node in  $G_n$  that is the fewest number of hops away from the most-likely superspreader in  $G_N$  (i.e., the optimal maximum likelihood estimate had this  $G_N$  been given entirely upfront to the contact tracer as has been first studied in [9]).

Given the data  $G_n$  harvested by contact tracing at the  $n$ -th stage, we have the following maximum-likelihood estimation (MLE) problem:

$$\hat{v} \in \arg \max_{v \in G_n \subseteq G_N \subseteq G} \mathbb{P}(G_n | v), \quad (1)$$

where  $\mathbb{P}(G_n | v)$  is the likelihood function and  $\hat{v}$  is the most likely superspreader of the outbreak. The key challenge is that  $G_N$  is unknown to the contact tracer who has to consider:

*Forward contact tracing:* How to construct the contact tracing network efficiently starting from a given index case?

*Backward contact tracing:* How to solve (1) to give the best instantaneous estimate of the superspreader given the data?

Answering both the forward and backward contact tracing jointly constitutes an iterative statistical inference process to track the most-likely superspreader in the entire epidemic network. Specifically, to answer the forward contact tracing problem, it is a natural idea to grow the contact tracing network

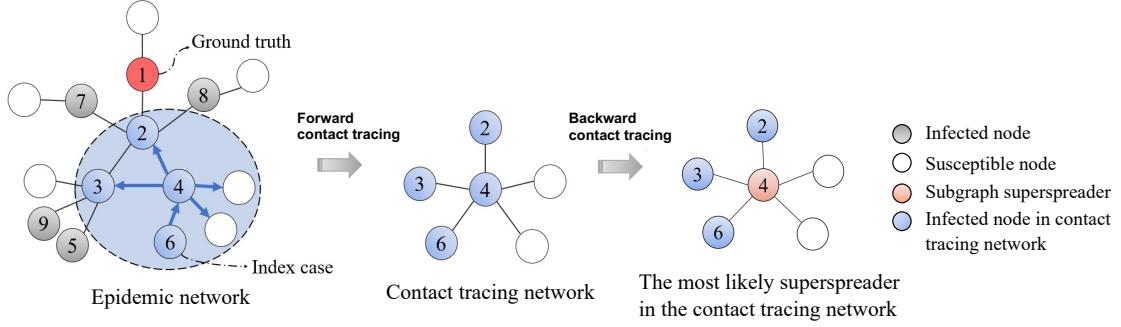


Fig. 2: Illustration of an epidemic network  $G_9$  with nine infections (shaded nodes) whose numbering indicates the infection order starts from the ground truth, i.e., the real superspreaders. The contact tracing network  $G_4$  (within a dotted circle) starting from the index case node  $v_6$  (blue arrows show the tracing directions) by forward contact tracing. The backward contact tracing is to find the node in  $G_9$  that is most likely to be the superspreaders.

with breadth-first search (BFS) or depth-first search (DFS) graph traversal algorithm from the index case. To answer the backward contact tracing problem, let us suppose that a given node  $v$  in  $G_n$  is assumed to be the superspreaders. Then, starting from that node, there are a number of possible ways to infect all the other nodes consistent with  $G_n$  harvested by contact tracing at the  $n$ -th stage. Even though  $G_N$  is unknown, it is reasonable for a contact tracer to assume a possible infection order in  $G_n$  by a *permitted permutation* by  $\sigma = \{v, v_1, v_2, \dots, v_{n-1}\}$ , and thus the problem in (1) can be equivalently expressed as:

$$v \in \arg \max_{v \in G_n} \sum_{\sigma \in \Omega(G_n | v)} \mathbb{P}(\sigma | v), \quad (2)$$

where  $\Omega(G_n | v)$  is the collection of all permitted permutations for  $G_n$  rooted at  $v$ , and  $\mathbb{P}(\sigma | v)$  is the probability of the permitted permutation  $\sigma$  with  $v$  as source.

Under the SI model, the probability of a susceptible node being infected next is uniformly distributed among all susceptible nodes at the boundary of  $G_n$ , and the probability of a permitted permutation is as follows:

$$\mathbb{P}(\sigma | v) = \prod_{i=2}^n \frac{\Phi_i(V)}{\sum_{j=1}^{i-1} d(v_j) - 2(i - \Phi_{i-1}(V) - 1)}, \quad (3)$$

where  $V$  denotes the node set of  $G_n$ ,  $d(v_i)$  is the degree of node  $v_i$  in  $G_n$ , and  $\Phi_i(V) = |e(v_i) \cap (\bigcup_{j=1}^{i-1} e(v_j))|$  with  $e(v_i)$  being the edge set of node  $v_i$ . If  $G_n$  is a general tree as a special case, then  $\Phi_i(V) = 1$ , for  $i = 1, 2, \dots, n$ , and the probability of a permitted permutation is given by [9]:

$$\mathbb{P}(\sigma | v) = \prod_{i=2}^n \frac{1}{\sum_{j=1}^{i-1} d(v_j) - 2(i - 2)}. \quad (4)$$

Coming back to the contact tracer who starts from the index case  $G_1$  and collects more data in a forward manner (i.e., enlarging  $G_n$  in (2)), the contact tracer also predicts the superspreaders for that instant by solving (1). Intuitively, as the contact tracing subgraph  $G_n$  grows, the contact tracer desires this prediction to be closer (in terms of the number of hops in  $G_N$ ) to the most-likely superspreaders in  $G_N$ . Taking this into account, how should  $G_n$  grow in *forward contact tracing*? We

propose to grow  $G_n$  using the BFS and DFS graph traversal algorithms [29], [30], which is described in detail in the next section.

### III. DIGITAL CONTACT TRACING BY BFS AND DFS

In this section, we detail interesting insights into tracing superspreaders in BFS tracing networks (using BFS traversal for forward contact tracing) and DFS tracing networks (using DFS traversal for forward contact tracing).

#### A. Backward Contact Tracing for BFS Tracing Networks

Firstly, we propose to grow  $G_n$  using the BFS graph traversal algorithm [29], [30].<sup>2</sup> Fig. 3 illustrates this with a tracer who starts from node  $v_a$ , and then moves to the node  $v_d$  (the most-likely superspreaders). Denote  $v_N^*$  and  $v_n^*$  as the approximate superspreaders obtained by estimator (2) in  $G_N$  (a general graph) and  $G_n$  (a rooted tree), respectively. Clearly,  $v_1^* = G_1$ . If  $N$  is fixed, we have the following result showing  $v_n^*$  approaches  $v_N^*$  for special cases of  $G_N$ .

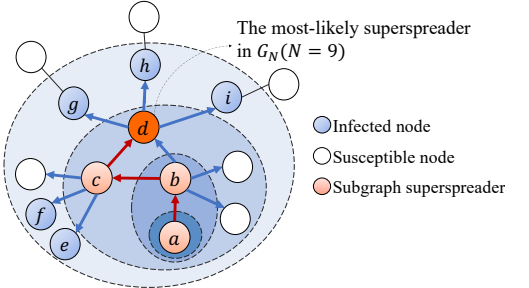


Fig. 3: As the contact tracing network grows from the index case  $v_a$  with BFS traversal, as ordered alphabetically  $\{a, b, c, \dots, i\}$ , the most-likely superspreaders computed by (2) in the contact tracing network moves closer to the most-likely superspreaders  $v_d$  in the epidemic network  $G_N$  (indicated by red arrows).

<sup>2</sup>The BFS algorithm yields a spanning tree, starting from a node  $u$ , of a graph  $G = (V, E)$  called a BFS Tree with complexity  $O(|V| + |E|)$  if, for each node, the path to  $u$  has the minimum number of hops ([30], Sec. 1.5.1, pp. 13). A distributed computation of this BFS Tree is given in [29].

**Theorem 1:** As the contact tracing network  $G_n$  grows and spans  $G_N$ ,  $v_n^*$  converges eventually to  $v_N^*$ . Specifically, if  $G_N$  is a  $d$ -regular tree, and there exists a node  $\bar{v}$  such that for any two leaf nodes  $v_{\text{leaf}}$  and  $u_{\text{leaf}}$  in  $G_N$ ,

$$|\text{dist}(v_{\text{leaf}}, \bar{v}) - \text{dist}(u_{\text{leaf}}, \bar{v})| \leq 1, \quad (5)$$

where  $\text{dist}(u, v)$  denotes the distance (i.e., number of hops) between node  $u$  and  $v$  in the graph, then the trajectory of  $v_n^*$  is exactly the shortest path from the index case  $v_1^*$  to  $v_N^*$  in  $G_N$ .

**Proof:** It is obvious that for any initial point  $v_1^* \in G_N$  from which  $G_n$  spreads,  $G_n$  covers  $G_N$  at most after  $N-1$  steps of BFS traversal. Therefore,  $v_n^*$  finally converges to  $v_N^*$ .

For any  $d$ -regular tree, finding the superspreaders by (2) is equivalent to finding its centroids [16]. Therefore,  $v_n^*$  is the centroid of  $G_n$ . Suppose the maximum size of the subtrees of  $G_n$  rooted at  $v_n^*$  is  $m$ , then for any node  $v_n^i$  with  $i$  hops away from  $v_n^*$ , the maximum size of the subtrees of  $G_n$  rooted at  $v_n^i$  is no less than  $m+i-1$ . After  $G_n$  growing within a BFS traversal step to generate  $G_{n+1}$ , the maximum size of the subtrees of  $G_{n+1}$  rooted at  $v_n^*$  either  $m$  or  $m+1$ , and the maximum size of the subtrees of  $G_{n+1}$  rooted at  $v_n^i$  is still no less than  $m+i-1$ . Therefore, the centroid  $v_{n+1}^*$  of  $G_{n+1}$  must be no more than 1 hop away from  $v_n^*$  in  $G_n$ , which is

$$\text{dist}(v_n^*, v_{n+1}^*) \leq 1. \quad (6)$$

On the other hand, since  $G_N$  is a  $d$ -regular tree satisfying (5), it is obvious that  $v_N^*$  is in the middle of the longest path of the tree and  $v_N^* = \bar{v}$ . Since any contact tracing subtree  $G_n$  growing with BFS traversal on  $G_N$  is still a  $d$ -regular tree satisfying (5), after  $G_n$  growing within a BFS traversal step to generate  $G_{n+1}$ , if  $G_n$  does not touch the boundary (i.e. the leaf node) of  $G_N$ , then  $v_n^* = v_{n+1}^*$ . When  $G_n$  touches the boundary of  $G_N$ , if  $v_n^* = v_N^*$ , then  $v_n^* = v_{n+1}^*$ . If  $\text{dist}(v_n^*, v_N^*) > 0$ , then  $v_N^*$  must not be in the paths from node  $v_n^*$  to the boundary that  $G_n$  touched as  $v_N^*$  satisfies (5). Furthermore, the next node adding into  $G_n$  to generate  $G_{n+1}$  in the next BFS traversal step must not be in the subtrees touching the boundary, which combining (6), leads to  $\text{dist}(v_{n+1}^*, v_N^*) \leq \text{dist}(v_n^*, v_N^*)$  when  $\text{dist}(v_n^*, v_N^*) > 0$ . Therefore,

$$\text{dist}(v_{n+1}^*, v_N^*) \leq \text{dist}(v_n^*, v_N^*). \quad (7)$$

Since  $v_n^*$  converges eventually to  $v_N^*$ , combining (6) and (7), we can conclude that the trajectory of  $v_n^*$  is exactly the shortest path from  $v_1^*$  to  $v_N^*$  in  $G_N$ . ■

**Corollary 1:** Let  $v_N^*$  and  $v_n^*$  denote the superspreaders obtained by the optimal estimator (2) in  $G_N$  and  $G_n$ , respectively. As the contact tracing network  $G_n$  grows, if for all  $n$  the  $G_n$  is a complete  $N$ -ary tree<sup>3</sup> when choosing  $v_n^*$  as the root, then the trajectory of  $v_n^*$  is exactly the shortest path from  $v_1^*$  to  $v_N^*$  in  $G_N$ .

**Proof:** If  $G_n$  is a complete  $N$ -ary tree, then  $|\text{dist}(v_{\text{leaf}}, v_n^*) - \text{dist}(u_{\text{leaf}}, v_n^*)| \leq 1$  for every  $v_{\text{leaf}}$  in  $G_n$ . From Theorem 1, we have that the trajectory of  $v_n^*$  is exactly the shortest path from  $v_1^*$  to  $v_N^*$  in  $G_N$ . ■

<sup>3</sup>A complete  $N$ -ary tree is an  $N$ -ary tree, and each of its levels must be full except for the bottom level. Moreover, if the bottom level is not full, then all nodes of the bottom level must be filled from left to right [31].

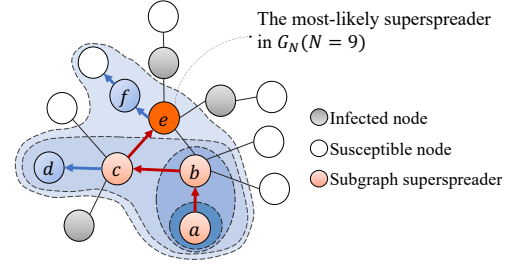


Fig. 4: As the contact tracing network grows from the index case  $v_a$  with DFS traversal, as ordered alphabetically  $\{a, b, c, \dots, f\}$ , the most-likely superspreader computed by (2) in the contact tracing network moves closer to the most-likely superspreader  $v_e$  in the epidemic network  $G_N$  (indicated by red arrows).

Mathematically, the forward contact tracing process yields a rooted tree  $G_n$ , whose node that solves (2) maximizes the sum of the permitted permutation probabilities. For special cases, Theorem 1 states that this maximizer is the graph centroid of  $G_n$ , and that it converges to the graph centroid of  $G_N$  when  $N$  is fixed (i.e., the graph centroid of a rooted subtree converges to that of a tree when the rooted tree  $G_n$  spans the entire graph  $G_N$ ).

### B. Backward Contact Tracing for DFS Tracing Networks

Now let us consider growing  $G_n$  with DFS<sup>4</sup> tracing strategy [30], which is illustrated in Fig. 4. Let  $S = (v_1^*, v_2^*, \dots, v_N^*)$  denote the sequence of all estimated superspreaders in  $G_n$  for  $n = 1, 2, \dots, N$  and  $X = (v^1, v^2, \dots, v^N)$  denote the sequence of nodes identified by the DFS tracing strategy. Hence the index case is  $v^1 = v_1^*$ . We categorize all consecutive pairs  $(v_i^*, v_{i+1}^*)$  in  $S$  into the following three types:

$$\begin{aligned} S_1 &= \{(v_i^*, v_{i+1}^*) | v_i^* = v_{i+1}^*\}, \\ S_2 &= \{(v_i^*, v_{i+1}^*) | v_i^* \neq v_{i+1}^* \text{ and } v_j^* \neq v_{i+1}^* \text{ for all } j < i\}, \\ S_3 &= \{(v_i^*, v_{i+1}^*) | v_i^* \neq v_{i+1}^* \text{ and } v_j^* = v_{i+1}^* \text{ for some } j < i\}. \end{aligned}$$

The first type  $S_1$  represents the estimated superspreader remains the same from  $n = i$  to  $n = i+1$ . The second type  $S_2$  implies that the node  $v_{i+1}^*$  is chosen to be the estimated superspreader for the first time. The third type  $S_3$  implies that  $v_{i+1}^*$  had been chosen as the estimated superspreader before. Denote the size of the three types of consecutive pairs by  $|S_1|$ ,  $|S_2|$  and  $|S_3|$ , respectively. Let  $T^v$  be a rooted tree of  $G_n$  rooted at  $v$  and denote the subtree of  $T^v$  rooted at  $u$  as  $T_u^v$  [16]. Then we introduce the following insights of the sequence  $S$  by considering  $S_1$ ,  $S_2$  and  $S_3$ .

**Lemma 1:** For any epidemic network  $G_N$ , we have  $|S_1| + |S_2| + |S_3| = N-1$ .

**Proof:** The size of  $S$  is  $N$ , so there are only  $N-1$  consecutive pairs in  $S$ . Moreover,  $S_1, S_2$  and  $S_3$  are mutually

<sup>4</sup>The DFS algorithm (i.e., the Trémaux's algorithm) for a finite, connected graph  $G = (V, E)$  also yields a spanning tree of  $G$ , which complexity is only  $O(|E|)$  ([30], Sec. 3.1.1, pp. 46).

exclusive. We can conclude that  $|S_1| + |S_2| + |S_3| = N - 1$ .  $\blacksquare$

**Lemma 2:** For any epidemic network  $G_N$ , we have  $S_1 \geq S_2 \geq S_3$

*Proof:* To prove  $|S_1| \geq |S_2| \geq |S_3|$ , we can observe that both type two and type three transitions must be followed by a type one transition, which means the size of type one transition is more than type two and type three. Moreover, each type three transition must come from a type two transition. Hence, we can conclude that  $|S_1| \geq |S_2| \geq |S_3|$ .  $\blacksquare$

**Theorem 2:** For any epidemic network  $G_N$ , if we apply DFS tracing strategy, then  $|S_3| \leq \log_2(N)$ .

*Proof:* Let  $S_3 = \{(v_{i_1}^*, v_{i_1+1}^*), (v_{i_2}^*, v_{i_2+1}^*), \dots, (v_{i_k}^*, v_{i_k+1}^*)\}$ , where  $k = |S_3|$ . Let  $U(v)$  denote the set of all children  $u$  of  $v$  and the subtree  $T_u^v$  is fully visited by the DFS strategy. To prove this theorem, we can show that  $2i_j \leq i_{j+1}$  for all  $j < k$ .

Given  $v^t = v$  and a consecutive pair  $(v_{j_1}^*, v_{j_1+1}^*) \in S_3$ , where  $v_{j_1}^* = v$ . If we treat the index case as the root of  $G_n$ , then there are two possible relations between  $v_{j_1}^*$  and  $v_{j_1+1}^*$ . The node  $v_{j_1}^*$  is either a child of  $v_{j_1+1}^*$  or  $v_{j_1}^*$  is the parent of  $v_{j_1+1}^*$ . If  $v = v_{j_1}^*$  is a child of  $v_{j_1+1}^*$ , then  $v_{j_1}^*$  is the last time that  $v$  is the estimated superspreaders due to the property of DFS traversal.

We first consider the case that  $v_{j_1}^*$  is the parent node of  $v_{j_1+1}^*$  and for the next  $(v = v_{j_2}^*, v_{j_2+1}^*) \in S_3$ ,  $v$  is still the parent of  $v_{j_2+1}^*$ . We assume that  $v_{j_1+1}^* = v^{d_1}$  and  $v_{j_2+1}^* = v^{d_2}$ . That is, the nodes  $v_{j_1+1}^*$  and  $v_{j_2+1}^*$  are the  $d_1$ th and the  $d_2$ th node visited by the DFS strategy. In this case, we have

$$j_1 + 1 = 2d_1 - 1.$$

Observe that  $v$  will not be the estimated superspreaders again until the subtree  $T_{v_{j_1+1}^*}^v \subseteq G_N$  is fully visited. Moreover, since  $(v = v_{j_2}^*, v_{j_2+1}^*) \in S_3$ , we have

$$\begin{aligned} j_2 + 1 &= 2d_2 - 1 \\ &> 2(j_1 + 1) - 1 \\ &= 2j_1 + 1, \end{aligned}$$

the second inequality follows by  $d_2 > j_1 + 1$ . For this case, we can conclude that if  $v$  was involved in more than one consecutive pairs say  $(v = v_{j_1}^*, v_{j_1+1}^*)$ , and  $(v = v_{j_2}^*, v_{j_2+1}^*)$  then the index  $j_2 > 2j_1$ .

For the second case, i.e.,  $v_{j_1}^*$  is the parent of  $v_{j_1+1}^*$  but for the next  $(v = v_{j_2}^*, v_{j_2+1}^*) \in S_3$ , the node  $v = v_{j_2}^*$  is a child of  $v_{j_2+1}^*$ . Since there is at most one such consecutive pair  $(v = v_{j_2}^*, v_{j_2+1}^*)$  for  $v$ , we do not need to bound such case.

Since the above two conclusions are true for any node, we can conclude that  $S_3 \leq \log_2(N)$ .  $\blacksquare$

The above theorem shows that if we apply the DFS tracing strategy to construct the contact tracing network, each node in the epidemic network  $G_N$  must not be re-detected as the superspreaders more than  $\log_2(N)$  times as the contact tracing network grows. Furthermore, from the above three observations, we can deduce that more than half of those consecutive pairs in  $S$  are type one, i.e., the estimated superspreaders will remain the same most of the time.

Now we discuss the performance of DFS and BFS tracing strategies. To quantify the performance, we introduce two measurements. The first one is the average error, which is defined by

$$\frac{1}{N} \sum_{i=1}^N \text{dist}(v_i^*, v_N^*). \quad (8)$$

The second one is the first detected time, i.e., the first time that the ground truth is computed as the estimated superspreaders. We can define the first detected time by

$$\min\{i | v_i^* = v_N^*\}. \quad (9)$$

The average error captures the overall performance during the contact tracing process. On the other hand, the first detected time is also an important measurement, since once the ground truth is computed as the estimated superspreaders, it is more likely to be the estimated superspreaders again in the future.

We found that the performance of two forward contact tracing strategies depends on the distance between the index case and the ground truth, i.e.,  $\text{dist}(v_1^*, v_N^*)$ . For example, let the epidemic network  $G_{10}$  be a 3-regular tree with six leaves. Assume that the index case is a leaf node, then the pair (average error, first detected time) is  $(0.7, 6)$  and  $(0.8, 7)$  for the DFS and BFS strategies, respectively. However, if the index case is exactly the ground truth, then the pair (average error, first detected time) should be  $(0.4, 0)$  and  $(0, 0)$  for the DFS and BFS strategies, respectively. In addition, when  $G_N$  is wide, i.e., each node has a large number of neighbors, using a BFS strategy for estimating superspreaders might be impractical, as the number of nodes to trace will explode. On the other hand, when  $G_N$  is deep, i.e., its diameter is large, DFS strategy might take longer than BFS strategy, as shown in Subsection V-B.

### C. Interpretation as Maze-Solving

Interestingly, solving (1) can be viewed as solving a maze where  $G_N$  is the maze topology. The solver (i.e., contact tracer) has no prior knowledge of this maze whose starting point and exit point correspond to  $v_1^*$  (initial index case) and  $v_N^*$  (the MLE had  $G_N$  been known a priori), respectively. The  $n$ th step in this maze corresponds to the centroid of a rooted tree  $G_n$ . Forward contact tracing and backward contact tracing are thus analogous to the process of maze traversal and maze exploration, respectively. Suppose a given abstract maze is a tree, then Theorem 1 illustrates that the BFS traversal yields the shortest path to solving the maze, and Theorem 2 describes that the DFS traversal yields a sequence of steps with less variance between steps. In addition to BFS and DFS traversal, there are other maze-solving algorithms in the literature, e.g., Tremaux's algorithms and the A\* search algorithm [30], that can inspire new contact tracing algorithms for solving (1).

## IV. DEEPTRECE: CONTACT TRACING WITH GNN

In general, solving problem (2) is computationally challenging when  $G_n$  is a large general graph. In this section, we leverage Graph Neural Network (GNN) to propose a backward

contact tracing algorithm to solve (2) with low computational complexity for an unknown  $G_N$  in large scale. Moreover, the proposed algorithm is online, i.e., the size  $N$  might be changing throughout the contact tracing process.

### A. Deep Learning on Graphs

As a deep learning model for processing unstructured data, GNN extracts graph features and information from the input data that are encoded as graphs. The learning mechanism of GNN is to iteratively aggregate features and information from neighboring nodes for each node in the input graphs. Aggregating information from neighbors is equivalent to a message passing process among nodes in a graph. Lastly, we update the values of learning parameters for either regression or classification tasks [32], [33]. For supervised machine learning, the training stage of GNN is important to capture simultaneously both the inherent statistical and graph topology features of the graph-structured input data.

Let  $\mathcal{G} = (\mathcal{V}, \mathcal{E})$  be a graph where each node in  $\mathcal{V}$  consists of  $m$  node features describing the given data point. Each edge  $(u, v) \in \mathcal{E}$  represents the connection between  $u$  and  $v$ . We now introduce the message passing mechanism in [23], [24] for updating feature vectors in each layer by aggregating information from neighboring nodes. At the  $l$ th layer of the GNN, the update rule of node  $v_i$  can be formulated as follow:

$$\begin{aligned} \mathbf{h}_{N_{\mathcal{G}}(v)}^{(l)} &= \text{AGGREGATE}^{(l)}(\{\mathbf{h}_u^{(l-1)} : u \in N_{\mathcal{G}}(v)\}), \\ \mathbf{h}_v^{(l)} &= \text{COMBINE}^{(l)}(\mathbf{h}_v^{(l-1)}, \mathbf{h}_{N_{\mathcal{G}}(v)}^{(l)}), \end{aligned} \quad (10)$$

where  $N_{\mathcal{G}}(v)$  denotes the set of neighbors of  $v \in \mathcal{G}$ ,  $\mathbf{h}_v^{(l)}$  is the updated node feature vector of  $v$  in the  $l$ th layer/iteration and  $\mathbf{h}_v^{(0)}$  denotes the initial feature vector of  $v$ .  $\mathbf{h}_{N_{\mathcal{G}}(v)}^{(l)}$  is an intermediate variable in the  $l$ th layer/iteration. The function  $\text{AGGREGATE}(\cdot)$  is an aggregation function, such as sum, mean, max-pooling and LSTM-pooling, to aggregate information from neighboring nodes. Likewise,  $\text{COMBINE}(\cdot)$  is a function, such as summation and concatenation, for updating the information of node  $v$  by combining information from its neighbors and its own information in the previous iteration. The design of the two functions in GNNs is crucial and can lead to different kinds of GNNs.

To motivate applying GNN to problem (2), there are two key computational aspects: the underlying epidemic network  $G_N$  is unknown to the contact tracer, and the size of  $G_N$  can be potentially massive. The role of GNN is thus to facilitate the computation of a (possibly suboptimal) solution to (2) when  $G_N$  is large. Due to the adaptability of GNNs, we can first generate a training set using small graphs (e.g., tens or hundreds of nodes) that are subgraphs of  $G_N$  and to augment descriptors with the structural features for each individual node of these graphs as the input data. The training stage requires correct labels (i.e., exact values of (3) to be associated with each of these small graphs. As the size of the graph grows, the computational cost of (3) becomes expensive. We may instead approximate (3) by sampling method to efficiently compute labels for the training data. Finally, we train the GNN model with the input subgraph data iteratively to update the neural

network hyperparameters as shown in Fig. 5. We explain this GNN architecture in details in the next subsection.

### B. Construction of Node Features

For GNN learning to be effective as part of a scalable algorithm to solve (2), the node features have to be carefully selected in order to extract the network topology information of the underlying epidemic network  $G_N$  for particular spreading models during the training stage. We now consider a few graph-theoretic properties like node degrees, the instantaneous infected proportion and boundary distances in graph. It is noted that the construction for all the node features only requires the computational complexity of  $O(N)$ . Let us describe these node features using Fig. 6 as a toy example as follows:

**Degree ratio:** This is the ratio of the degree of a node  $v_i$  to the sum of the degrees of all the nodes in the network:

$$r(v_i) = d(v_i) / \sum_{j=1}^n d(v_j),$$

where  $d(v_i)$  is the degree of node  $v$ . For example, the degree ratio of nodes  $v_1, v_2, v_3, v_4$ , and  $v_5$  in Fig. 6 are  $\frac{1}{12}, \frac{1}{8}, \frac{1}{6}, \frac{1}{8}$  and  $\frac{1}{6}$ , respectively. This node feature is straightforward to be considered as it plays an important role in calculating the permitted permutation probability in (3).

**Infected proportion:** This is the ratio of the number of infected neighbors of a node  $v_i$  to the number of all its neighbors:

$$\hat{r}(v_i) = \frac{\hat{d}(v_i)}{d(v_i)},$$

where  $\hat{d}(v_i)$  is the number of infected neighbors of the node  $v_i$ . For example, the number of infected neighbors of nodes  $v_1, v_2, v_3, v_4$ , and  $v_5$  in Fig. 6 are 1, 1, 4, 1 and 1. Then the infected proportion of nodes  $v_1, v_2, v_3, v_4$ , and  $v_5$  are  $\frac{1}{2}, \frac{1}{3}, 1, \frac{1}{3}$ , and  $\frac{1}{4}$ , respectively. Intuitively, a node with a lower infected proportion has a smaller probability of being the source.

**Boundary distance ratio:** This is the ratio of the shortest distance from the node  $v_i$  to the farthest leaf node at the network boundary, as shown in Fig. 6, and given by

$$\check{r}(v_i) = \frac{b(v_i)}{\max_{v_j \in G_n} b(v_j)},$$

where  $b(v_j)$  denotes the boundary distance of node  $v_j$ . For example, the boundary distances of node  $v_1, v_2, v_4$  and  $v_5$  in Fig. 6 are 2, and the boundary distances of node  $v_3$  is 3, so the boundary distance ratio of nodes  $v_1, v_2, v_3, v_4$  and  $v_5$  are  $\frac{2}{3}, \frac{2}{3}, 1, \frac{2}{3}$  and  $\frac{2}{3}$ , respectively. As shown in (2), finding the superspreader also requires the information of the size of the collection of all permitted permutations  $\Omega(G_n|v)$ . Choosing a node with a higher boundary distance ratio to be the source usually leads to a larger permitted permutation collection. For example, there are 24 permitted permutations when choosing node  $v_3$  to be the source, but only 6 permitted permutations if choosing node  $v_1, v_2, v_4$  or  $v_5$  to be the source.

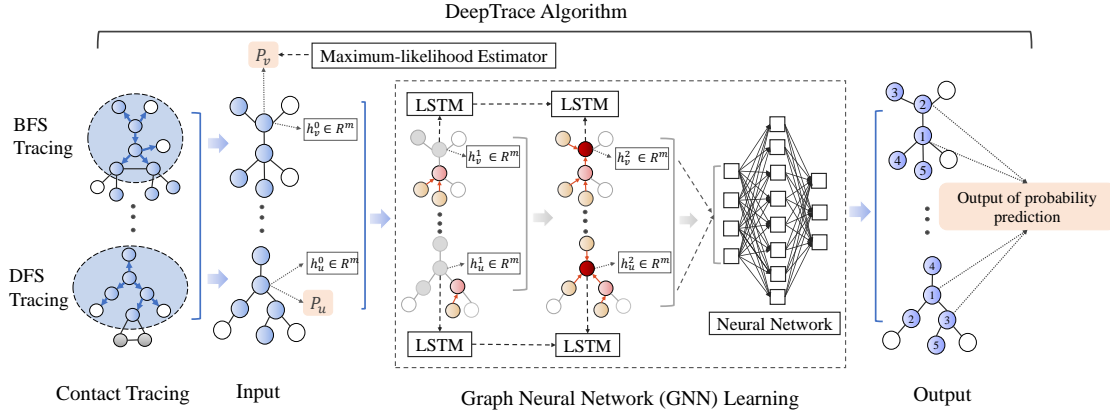


Fig. 5: The overall architecture of the DeepTrace algorithm using GNN with the input of a number of small-scale networks which can be obtained by using the BFS and DFS search methods and whose nodes have each the structural features and a training label, which is the permitted permutation probability. The supervised learning is carried out using GraphSage with LSTM aggregators.

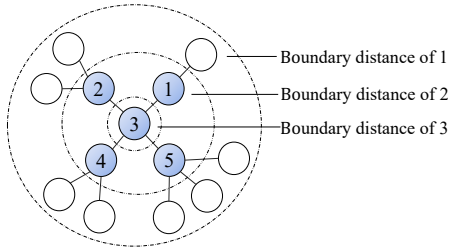


Fig. 6: An example of a given epidemic network illustrating the boundary distance for each node.

### C. DeepTrace with GNN

Now we propose to solve problem (2) for backward contact tracing in the epidemic network  $G_N$  by using GraphSage in [33], a popular inductive GNN model which can be adapted to different size of networks. For the growing contact tracing network  $G_n$ , we construct our GNN model with the LSTM [34] aggregator for aggregating information from the neighbors of a node and the ReLU function [34] for combining information of the node and its aggregated information. The  $l$ th layer of GNN is as follows:

$$\begin{aligned} \mathbf{h}_{N_{G_n}(v)}^{(l)} &= \text{LSTM}(\{\hat{\mathbf{w}}^{(l-1)}, \mathbf{h}_u^{(l-1)} : u \in N_{G_n}(v)\}), \\ \mathbf{h}_v^{(l)} &= \max(0, \check{\mathbf{w}}^{(l)} \cdot [\mathbf{h}_v^{(l-1)}; \mathbf{h}_{N_{G_n}(v)}^{(l)}]), \end{aligned} \quad (11)$$

where  $\hat{\mathbf{w}}^{(l)}$  and  $\check{\mathbf{w}}^{(l)}$  are the learning parameters in the LSTM aggregators and combination function, respectively. The initial node feature vector is  $\mathbf{h}_v^{(0)} = [r(v), \hat{r}(v), \hat{r}(v)]^T$  for  $v \in G_n$ , which we discuss in Subsection IV-B. We first prove the effectiveness of backward contact tracing with the GNN model (11) in the following Theorem 3.

*Theorem 3:* For a given epidemic network  $G_n = (V, E)$ , denote  $\text{diam}(G_n)$  as the diameter of  $G_n$ , and define each layer of the GNN model by (11). Then for  $\forall \epsilon > 0$  there exist a parameter setting  $(\hat{\mathbf{w}}^*, \check{\mathbf{w}}^*)$  in (11) with at most

$$L = \text{diam}(G_n) + 1 \text{ layers such that}$$

$$|\mathbf{h}_v^{(L)} - \mathbb{P}(G_n|v)| < \epsilon, \forall v \in V.$$

*Proof:* As shown in (2), solving problem (1) needs the information of all the permitted permutations for all the nodes in  $G_n$ . Since a newly infected node can only be infected by one of its infected neighbors,  $v_{i+1}$  must be the neighbor of  $v_i$  in any permitted permutation  $\sigma$ , and thus calculating  $p(\sigma|v)$  with (3) is actually a recursive process of aggregating the information of degree  $d(v_l)$  and  $\Phi_l(V)$  from the  $l$ th layer's neighbors of node  $v$  in  $\sigma$ , which can be expressed as

$$\mathbb{P}^{(l)}(\sigma|v) = \sum_{u \in N_G(v)} f(\mathbb{P}^{(l-1)}(\sigma|v), \mathbb{P}^{(l-1)}(\sigma|u)), \quad (12)$$

with  $\mathbb{P}^{(l)}(\sigma|v)|_{l=1} = 1/d(v)$ . Therefore, it is a recursive iteration to calculate  $\sum_{\sigma \in \Omega(G_n|v)} \mathbb{P}(\sigma|v)$  to aggregate the information of degree  $d(v_l)$  and  $\Phi_l(V)$  from its  $l$ th layer's neighbors in all  $\sigma \in \Omega(G_n|v)$ , which can be shown as

$$\begin{aligned} &\mathbb{P}^{(l)}(G_n|v) \\ &= \sum_{\sigma \in \Omega(G_n|v)} \sum_{u \in N_G(v)} f(\mathbb{P}^{(l-1)}(\sigma|v), \mathbb{P}^{(l-1)}(\sigma|u)) \\ &= \sum_{u \in N_G(v)} g(\mathbb{P}^{(l-1)}(G_n|v), \mathbb{P}^{(l-1)}(G_n|u)). \end{aligned} \quad (13)$$

The (13) demonstrates the process of iterative aggregation to calculate  $\mathbb{P}(G_n|v)$  for node  $v$ . Since  $G$  is connected, the shortest distance between any two nodes satisfies  $\text{dist}(u, v) \leq \text{diam}(G)$ . Then after  $\text{diam}(G)$  steps of aggregation and combination, each node can obtain the feature information of all nodes in the graph. Furthermore, it is not difficult to see that both  $f(\cdot)$  and  $g(\cdot)$  are continuous functions. Therefore, according to the universal approximation theorem, it can be approximated to an arbitrary degree of precision by standard multilayer perceptron with hidden layers and non-constant monotonically increasing activation functions [35]. ■

Since obtaining the labeled datasets for training (11) is computationally challenging, in order to tune the learning

parameters in (11), we conduct a two-phase training in a supervised manner: a pre-training phase and a fine-tuning phase. In particular, we first pre-train (11) using a dataset of contact tracing networks with approximations of  $\mathbb{P}(G_n|v)$  as labels for each node. This dataset can be easily obtained as described in Subsection IV-D. Then, we continuously fine-tune the learning parameters in the pre-trained model using other datasets of contact tracing networks with exact values of  $\mathbb{P}(G_n|v)$  as labels of each node. These datasets can be the special cases of the contact tracing networks (i.e.  $d$ -regular graphs in [9], [16]) and smaller-scale contact tracing subgraphs in the early tracing stages. Then we can use the fine-tuned model for larger contact tracing subgraphs. According to this workflow, we propose DeepTrace, the GNN-based learning algorithm, as the following Algorithm 1.

---

**Algorithm 1:** DeepTrace

---

**Input:** The index case (i.e.,  $G_1$ ); the GNN model defined in (11) with randomly initialized parameters.

**Output:** The prediction of probability as source for each node in the contact tracing network.

Step 1: Pre-train the GNN model using contact tracing networks with node labels as the approximations of  $\tilde{\mathbb{P}}(G_n|v)$  in (15).

Step 2: Generate the contact tracing network  $G_n$  using the BFS or DFS search strategy at the  $n$ -th stage;

Step 3: Construct the structure features  $\mathbf{h}_v^0 = [r(v), \hat{r}(v), \hat{r}(v)]^T$  for each node in  $G_n$  according to Subsection IV-B;

Step 4: Fine-tune the GNN model using contact tracing networks with node labels as the exact values of  $\mathbb{P}(G_n|v)$ .

Step 5: Predict the source probability for each node in  $G_n$  using the trained GNN model in Step 4. Go to Step 2 and repeat for  $n + 1$ .

---

#### D. Training Process with Supervised Learning

To train the GNN model in DeepTrace during the two-phase training process, we define the loss functions for the pre-training and fine-tuning phase, respectively, as follows:

$$L_p(\hat{\mathbf{w}}, \check{\mathbf{w}}, v | v \in G_n) \\ = \sum_{v \in G_n} |\log(\tilde{\mathbb{P}}(G_n|v)) - \mathbf{h}_v^{(L)}(\hat{\mathbf{w}}, \check{\mathbf{w}})|^2,$$

and

$$L_f(\hat{\mathbf{w}}, \check{\mathbf{w}}, v | v \in G_n) \\ = \sum_{v \in G_n} |\log(\mathbb{P}(G_n|v)) - \mathbf{h}_v^{(L)}(\hat{\mathbf{w}}, \check{\mathbf{w}})|^2,$$

where  $\tilde{\mathbb{P}}(G_n|v)$  is the approximation of  $\mathbb{P}(G_n|v)$ ,  $\hat{\mathbf{w}} = (\hat{\mathbf{w}}^{(1)}, \dots, \hat{\mathbf{w}}^{(L)})$  and  $\check{\mathbf{w}} = (\check{\mathbf{w}}^{(1)}, \dots, \check{\mathbf{w}}^{(L)})$ , and we take a logarithm of likelihood probabilities of nodes, so as to avoid arithmetic underflow as the values of likelihood probabilities

might be very small in magnitude as the epidemic network grows.

Next, we describe how to construct the training data sets for pre-training and fine-tuning the GNN model, respectively.

1) *Data Annotator for Pre-training:* For the labeled training data in the pre-training phase, we can use an approximate estimator of (1) to obtain  $\tilde{\mathbb{P}}(G_n|v)$  for each node  $v$  in the epidemic networks without spending too much time or effort.

When the epidemic networks are degree-irregular trees, the ML estimator in (1) attempts to calculate the sum of all probabilities of permitted permutations. It is observed that (1) can be further written as

$$v \in \arg \max_{v \in G_n} \tilde{\mathbb{P}}(G_n|v) |\Omega(G_n|v)|, \quad (14)$$

where  $\tilde{\mathbb{P}}(G_n|v)$  is the average of the probabilities of all permitted permutations. We can easily calculate  $|\Omega(G_n|v)|$  by a message-passing algorithm in [36] with time complexity  $\mathcal{O}(N)$ , but it is challenging to obtain the exact value of  $\tilde{\mathbb{P}}(G_n|v)$  since we still need to find out all the permitted permutations of  $G_n$  and their corresponding probabilities. Therefore, we randomly pick a small sample of the permitted permutations, which is denoted by  $\tilde{\Omega}(G_n|v)$ , and then we take the average of their probabilities as the approximation to  $\tilde{\mathbb{P}}(G_n|v)$ . Hence, the approximate MLE problem is as follows:

$$\hat{v} \in \arg \max_{v \in G_n} \frac{1}{|\tilde{\Omega}(G_n|v)|} \sum_{\sigma \in \tilde{\Omega}(G_n|v)} \mathbb{P}(\sigma|v) |\Omega(G_n|v)| \\ = \arg \max_{v \in G_n} \tilde{\mathbb{P}}(G_n|v). \quad (15)$$

2) *Data Annotator for Fine-tuning:* Since we already have a rough GNN model after pre-training, we can further refine the model with a small amount of high-quality data (i.e., the data of epidemic networks with exact likelihood probability as source for each node in the networks).

To construct the labeled data with exact likelihood probability for fine-tuning, a natural idea is to calculate the likelihood probability of each node directly by combining (2) and (3). In addition, we can also construct some data samples that are easy to obtain exact likelihood probabilities, such as the  $d$ -regular tree. Since the probabilities of all permitted permutations are identical, from (14) it is easy to see that the likelihood probability for a node in a  $d$ -regular tree by (2) is proportional to its centrality [16], which can be calculated by a message-passing algorithm in [16].

## V. PERFORMANCE EVALUATION

In this section, we first provide simulation results on the performance of the approximate ML estimator (15). Then we demonstrate the effectiveness of the DeepTrace algorithm on both synthetic networks and real-world networks based on real COVID-19 contact tracing data in Hong Kong and Taiwan. The data and implementation code for our experiments can be found in <https://github.com/convexsoft>.

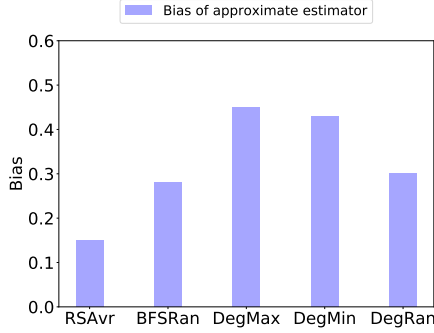


Fig. 7: The biases of different approximation estimators with respect to the actual average of all permutation probabilities, as defined in (16).

#### A. Approximate Estimator for Synthetic Networks

We first give some simulation results of the approximate estimator (15) on some synthetic networks. We generate a thousand synthetic networks, including the Erdős Rényi networks, Barabási Albert networks, Watts-Strogatz networks and random networks [37], each having about 250 nodes. Then we simulate infection in these networks to obtain synthetic epidemic networks. To do this, we randomly select a node on each network as the superspreader and then spread the infection under the SI model. When 20% of the nodes are infected, we stop the spreading simulation, and then apply (15) to these synthetic epidemic networks to evaluate its performance.

We evaluate the approximate estimator (15) in the performance of approximating the actual average probability  $\bar{\mathbb{P}}(G_n|v)$ , using the bias defined as

$$\text{bias} = \left| \frac{\log\left(\frac{1}{|\Omega(G_n|v)|} \sum_{\sigma \in \Omega(G_n|v)} \mathbb{P}(\sigma|v)\right) - \log \bar{\mathbb{P}}(G_n|v)}{\log \bar{\mathbb{P}}(G_n|v)} \right| \times 100\%. \quad (16)$$

Our baseline comparison is a heuristic given in [9] in which the probability of a permutation corresponding to a randomly selected BFS traversal on the entire  $G_N$  is used to approximate every permitted permutation in  $G_n$ , which is

$$\hat{v} \in \arg \max_{v' \in G_n} \mathbb{P}(\sigma_{v'}|v) |\Omega(G_n|v)|, \quad (17)$$

where  $\sigma_{v'}$  is one of the permitted permutations corresponding to a random BFS traversal with node  $v$  as the superspreader. We compare five methods for bias approximation, as shown in Fig. 7. The "RSAvr", "BFSRan", "DegMax", "DegMin", and "DegRan" in the X-axis denote the average probability of the randomly sampled permitted permutation in (15), the probability of a random BFS permitted permutation, the maximum probability of all permitted permutations, the minimum probability of all permitted permutations, and the probability of a randomly selected permitted permutation, respectively. We can observe that the average probability of the randomly sampled permitted permutation for (15) performs well with an average bias of about 15%.

#### B. Contact Tracing with DeepTrace for Synthetic Networks

1) *Backward Contract Tracing with DeepTrace*: Now let us evaluate the performance of the DeepTrace algorithm in estimating the superspreaders in epidemic networks. We conduct a two-phase supervised learning that consists of a pre-training and a fine-tuning phase. Similar to Subsection V-A, we generate 500, 250 and 250 synthetic epidemic networks as training datasets for the pre-training, fine-tuning and testing the GNN model. These datasets have approximately 50 ~ 1000, 50, and 50 ~ 1000 infected nodes in the synthetic epidemic networks, respectively. We obtain the initial feature vector  $\mathbf{h}_v^{(0)} = [r(v), \hat{r}(v), \hat{r}'(v)]^T$  for each node in these networks according to the analysis in Subsection IV-B. For the training data used in the pre-training phase, we label each node with  $\tilde{\mathbb{P}}(G_n|v)$  in (15), while for the network data used in the fine-tuning phase and testing, we label each node with the exact probability  $\mathbb{P}(G_n|v)$  in (1). A summary of these datasets is shown in the TABLE I.

Data size	Nodes	Edges	Features	Labels	Task
500	50~1000	49~999	$\mathbf{h}_v^0$	$\log(\tilde{\mathbb{P}}(G_n v))$	Pre-training
250	$\approx 50$	$\approx 50$	$\mathbf{h}_v^0$	$\log(\mathbb{P}(G_n v))$	Fine-tuning
250	50~1000	49~999	$\mathbf{h}_v^0$	$\log(\mathbb{P}(G_n v))$	Testing

TABLE I: The summary of the datasets of the synthetic epidemic networks for pre-training, fine-tuning and testing when training the GNN in DeepTrace.

Then we pre-train and fine-tune the GNN model in DeepTrace both for 150 epochs, and use the bias defined as follows to evaluate the performance of the trained GNN in the two-phase training process:

$$\text{bias}' = \left| \frac{\log \mathbb{P}'(G_n|v) - \log \bar{\mathbb{P}}(G_n|v)}{\log \bar{\mathbb{P}}(G_n|v)} \right| \times 100\%, \quad (18)$$

where  $\log \mathbb{P}'(G_n|v)$  is the output of the GNN in DeepTrace. The results of pre-training and fine-tuning are shown in Fig. 8 (a) and Fig. 8 (b), respectively. From the results we can see that the GNN after pre-training achieves great approximate probability, and fine-tuning further improves the performance of the pre-trained GNN. Furthermore, we evaluate the performance of the trained GNN by the top- $k$  accuracy. Here top- $k$  means that the approximate superspreader detected by the trained GNN is in the set of  $k$  nodes with the highest probability as superspreaders. For example, if the approximate superspreader detected by the trained GNN is top-0, then it indicates that this approximate superspreader is the most likely superspreader. The results of the top- $k$  accuracy for the testing dataset in the phases of pre-training and fine-tuning are shown in Fig. 8 (c) and Fig. 8 (d), respectively.

Next, we measure the generalization ability of the DeepTrace algorithm, that is, validate the effectiveness of the GNN trained by the small-scale epidemic networks on the larger epidemic networks. We additionally construct 6 validation datasets of synthetic networks, each with 100 networks, and the numbers of nodes in each set of networks are 50, 100, 200, 500, 1000, and 2500, respectively. Also, we simulate the infection to obtain the epidemic networks according

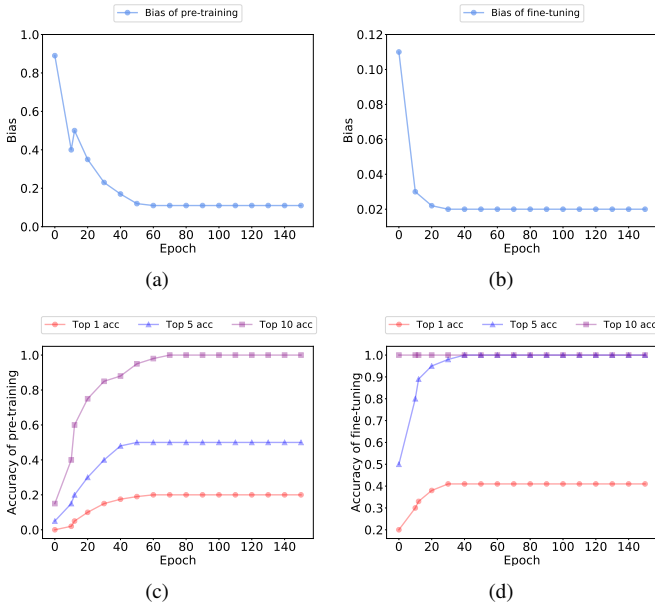


Fig. 8: Illustration of the results of the GNN model. (a) and (b) shows the bias trajectory between the approximate likelihood probability obtained by the GNN model and the accurate likelihood probability for the testing dataset in the pre-training and the fine-tuning phase, respectively. (c) and (d) shows the trajectories of top 1, top 5 and top 10 accuracy for the testing dataset in the pre-training and fine-tuning phase, respectively.

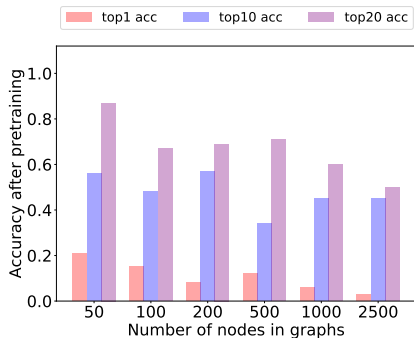


Fig. 9: The top-1, top-10 and top-20 prediction accuracy for validation datasets after pre-training in DeepTrace.

to the procedure in Subsection V-A. Then we evaluate the performance of the trained GNN on these validation datasets by the top- $k$  accuracy. After training for 150 epochs, we use the top-1, top-10 and top-20 prediction accuracy for each validation dataset. Fig. 9 and Fig. 10 show the results of the pre-training and fine-tuning process, which indicates that the trend of the accuracy does not decay sharply as the number of nodes in the networks increases. This means that the model trained with small-scale networks still works in the larger networks to some extend. Therefore, it is effective to transfer the trained model into larger networks to accelerate the speed of detecting the superspreader.

2) *Comparison Between BFS and DFS Tracing Networks:* Now we compare the effectiveness of choosing BFS and DFS tracing strategies for forward contact tracing in epidemic

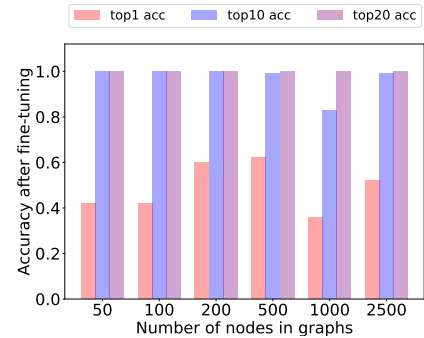


Fig. 10: The top-1, top-10 and top-20 prediction accuracy for validation datasets after fine-tuning in DeepTrace.

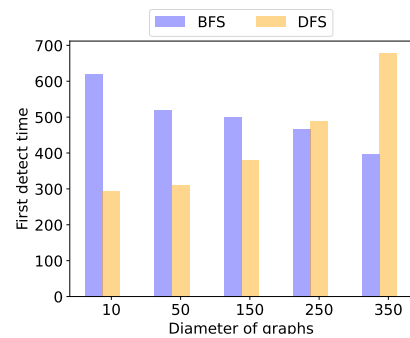


Fig. 11: The first detected time for backward contact tracing on contact tracing networks using BFS and DFS tracing strategies on underlying epidemic networks with different diameters.

networks with different network structures. Here we mainly consider the structure of network depth, i.e., the diameter of network. We first generate a new dataset of synthetic networks, each of which has 1500 nodes and different diameters ranging from 10 to 350. Then we partition these networks into 5 groups according to their diameters. Also, to obtain synthetic epidemic networks, we simulate the virus spreading in these synthetic networks by randomly selecting a node on each network as the superspreader and then spreading the virus under the SI model. When 20% of the nodes are infected, we stop the spreading simulation. Then we use BFS and DFS for forward contact tracing in these epidemic networks to obtain the contact tracing networks, respectively.

After that, we apply the trained GNN model in DeepTrace to these contact tracing networks to detect their most likely superspreaders. To compare the performance of the BFS and DFS tracing strategies, we use the first detected time defined in (9). The results are shown in Fig. 11, from which we can see that as the diameter of the networks grows, the first detected time of the BFS tracing strategy decreases while it increases for the DFS tracing strategy. This provides us some guidance in choosing the BFS and DFS tracing strategies for forward contact tracing when we have prior knowledge of the underlying epidemic networks.

### C. Contact Tracing with DeepTrace for COVID-19 Pandemic in Hong Kong

In this section, we conduct experiments on COVID-19 epidemic data in Hong Kong to evaluate the performance of the DeepTrace algorithm. We refer to  $G_n$  as the epidemic network in the following, where nodes in  $G_n$  represent confirmed cases and each edge in  $G_n$  implies that there is a connection between two end nodes of the edge. Moreover, the number on each node indicates the infection order, i.e., the node labeled 1 is the actual superspreader in the epidemic network. We compare the DeepTrace algorithm to estimators provided by (15) and (1). Since the size of these two clusters is not too large, the computation of the ML estimator (1) is tractable.

1) *COVID-19 Temple Cluster in Hong Kong*: We first consider the Buddhist temple cluster of coronavirus infections in Hong Kong [38]. This cluster occurred in February 2020, leading to 19 confirmed cases. Fig. 12 illustrates the epidemic network of this infected cluster.

To approximate the superspreader, we apply the DeepTrace algorithm to this network. Then we compute the distance between the approximate superspreader and the ground truth  $v_1$  to verify the performance of our algorithm. The result is shown in Fig. 12, where the red node is the ground truth, and the purple node is the approximate superspreader obtained by the estimator (15), estimator (1), and the DeepTrace algorithm. Due to the tree structure, we can see that all estimators predict the same vertex  $v_2$  which is one hop from the ground truth.

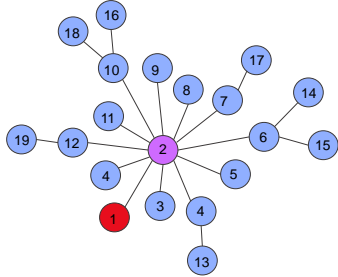


Fig. 12: The COVID-19 temple cluster in Hong Kong in February 2020. The red node is the real superspreader, and the purple node is the approximate superspreader obtained by the approximate estimator (15), the approximate superspreader obtained by the DeepTrace and the estimator (1).

2) *COVID-19 Wedding Cluster in Hong Kong*: In March 2020, a COVID-19 superspreading cluster broke out in a wedding party in Hong Kong, which leads to a group of 23 confirmed cases as shown in Fig. 13. This cluster was linked to the wedding and a preceding social event [38].

Similarly, we apply the DeepTrace algorithm to this epidemic network to approximate the superspreader. The results are shown in Fig. 13, where the red node is the ground truth, the yellow node is the approximate superspreader obtained by the estimator (15), and the purple node is the approximate superspreader obtained by the DeepTrace and the ML estimator (1). In this case, we can observe that the approximate superspreader examined by DeepTrace is as good as the ML estimator (1), and outperforms the estimator (15).

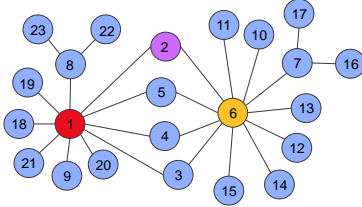


Fig. 13: The epidemic network of the wedding cluster in Hong Kong in March 2020, where the red node is the actual superspreader. The yellow node is the estimator obtained by (15), and the purple node is the approximate superspreader obtained by our DeepTrace and the estimator (1).

### D. Contact Tracing with DeepTrace for COVID-19 Pandemic in Taiwan

In addition to the Hong Kong COVID-19 data, we conduct one more experiment using COVID-19 epidemic data of Taiwan from September 2020 to March 2021 in [39], from which we randomly sample 100 days of data and construct epidemic networks for each day's data. The epidemic networks consist of 488 to 1036 cases. We first apply the DeepTrace to detect the most likely superspreaders in the epidemic network, and compare the accuracy to those with the approximate probabilities obtained from estimator (15). The top-1, top-5, top-10 and top-20 prediction accuracy results are shown in TABLE II.

Top- $k$	Top-1	Top-5	Top-10	Top-20
Accuracy	0.49	0.87	0.98	1.00

TABLE II: The top-1, top-5, top-10 and top-20 prediction accuracy of DeepTrace on the real COVID-19 contact tracing network in Taiwan.

To visualize the network structure, we select one snapshot of the contact tracing network on 1 September 2020, and then simulate contact tracing with one tracer starting from one initial node. As the contact tracing network grows, the final results of approximating the superspreaders are shown in Fig. 14. The red node, orange node, purple node and yellow node in Fig. 14 are the superspreaders obtained by the ML estimator (2), DeepTrace, approximate estimator (15), and the random BFS estimator in [14], with the hops from the index case as 3, 4, 7 and 11, respectively. Therefore, the DeepTrace algorithm also performs well in real epidemic networks.

## VI. CONCLUSION

In this paper, we have formulated a backward contact tracing problem as a maximum likelihood estimation of the epidemic source that finds applications in locating the superspreader of epidemic spreading. Given an index case, the contact tracer can traverse the epidemic network in a breadth-first search or depth-first search manner to compute the graph center of the instantaneous contact tracing subgraph that is shown to converge eventually to the optimal likelihood estimate for special graph topology. We have proposed a deep learning algorithm,

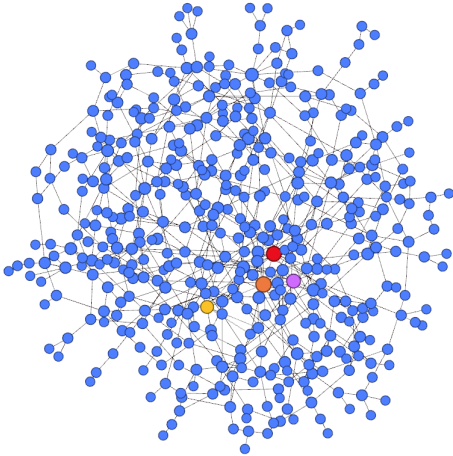


Fig. 14: The COVID-19 epidemic network in Taiwan on 1 September 2020, in which the red node, orange node, purple node and yellow node are the superspreaders obtained by the ML estimator (2), DeepTrace, approximate estimator (15), and the random BFS estimator in [14], respectively.

which we named DeepTrace, based on graph neural network supervised learning for general and potentially massive graphs using message passing. Furthermore, we have validated the effectiveness of our methodology by modeling and analyzing real data of COVID-19 superspreading events in Hong Kong and Taiwan, demonstrating that our contact tracing algorithm can outperform the existing contact tracing heuristic.

## REFERENCES

- [1] S. Landau, *People Count: Contact-Tracing Apps and Public Health*. MIT Press, 2021.
- [2] Y. Bengio, P. Gupta, T. Maharaj, N. Rahaman, M. Weiss, T. Deleu, E. B. Muller, M. Qu, P.-l. St-charles, O. Bilaniuk *et al.*, “Predicting infectiousness for proactive contact tracing,” in *Proceedings of the International Conference on Learning Representations*, 2021.
- [3] D. Leith and S. Farrell, “A measurement-based study of the privacy of Europe’s COVID-19 contact tracing apps,” in *Proceedings of the IEEE International Conference on Computer Communications*, 2021.
- [4] H. Stevens and M. B. Haines, “Tracetogther: pandemic response, democracy, and technology,” *East Asian Science, Technology and Society*, vol. 14, no. 3, pp. 523–532, 2020.
- [5] G. Cencetti, G. Santin, A. Longa, E. Piganis, A. Barrat, C. Cattuto, S. Lehmann, M. Salathe, and B. Lepri, “Digital proximity tracing on empirical contact networks for pandemic control,” *Nature Communications*, vol. 12, no. 1, pp. 1–12, 2021.
- [6] S. Kojaku, L. Hébert-Dufresne, E. Mones, S. Lehmann, and Y.-Y. Ahn, “The effectiveness of backward contact tracing in networks,” *Nature Physics*, vol. 17, no. 5, pp. 652–658, 2021.
- [7] W. J. Bradshaw, E. C. Alley, J. H. Huggins, A. L. Lloyd, and K. M. Esveld, “Bidirectional contact tracing could dramatically improve COVID-19 control,” *Nature Communications*, vol. 12, no. 1, pp. 1–9, 2021.
- [8] S. Chen, P.-D. Yu, C. W. Tan, and H. V. Poor, “Identifying the superspreader in proactive backward contact tracing by deep learning,” in *Proceedings of the 56th Annual Conference on Information Sciences and Systems (CISS)*, 2022.
- [9] D. Shah and T. Zaman, “Rumors in a network: Who’s the culprit?” *IEEE Transactions on Information Theory*, vol. 57, no. 8, pp. 5163–5181, 2011.
- [10] N. Bailey, *The Mathematical Theory of Infectious Diseases and Its Applications*. Hafner Press, 1975.
- [11] N. C. Grassly and C. Fraser, “Mathematical models of infectious disease transmission,” *Nature Reviews Microbiology*, vol. 6, no. 6, pp. 477–487, 2008.
- [12] Y.-C. Chen, P.-E. Lu, C.-S. Chang, and T.-H. Liu, “A time-dependent SIR model for COVID-19 with undetectable infected persons,” *IEEE Transactions on Network Science and Engineering*, vol. 7, no. 4, pp. 3279–3294, 2020.
- [13] R. Eletreby, Y. Zhuang, K. M. Carley, O. Yağan, and H. V. Poor, “The effects of evolutionary adaptations on spreading processes in complex networks,” vol. 117, no. 11, 2020, p. 5664.
- [14] D. Shah and T. Zaman, “Rumor centrality: a universal source detector,” in *Proceedings of ACM SIGMETRICS/PERFORMANCE joint international conference on Measurement and Modeling of Computer Systems*, 2012.
- [15] B. Zelinka, “Medians and peripherians of trees,” *Archivum Mathematicum*, vol. 4, no. 2, pp. 87–95, 1968.
- [16] P. D. Yu, C. W. Tan, and H. L. Fu, “Averting cascading failures in networked infrastructures: Poset-constrained graph algorithms,” *IEEE Journal of Selected Topics in Signal Processing*, vol. 12, no. 4, pp. 733–748, 2018.
- [17] L. Vassio, F. Fagnani, P. Frasca, and A. Ozdaglar, “Message passing optimization of harmonic influence centrality,” *IEEE Transactions on Control of Network Systems*, vol. 1, no. 1, pp. 109–120, 2014.
- [18] N. Karamchandani and M. Franceschetti, “Rumor source detection under probabilistic sampling,” in *Proceedings of the IEEE International Symposium on Information Theory (ISIT)*, 2013.
- [19] Z. Wang, W. Dong, W. Zhang, and C. W. Tan, “Rumor source detection with multiple observations: Fundamental limits and algorithms,” in *Proceedings of the ACM SIGMETRICS Performance Evaluation Review*, 2014.
- [20] W. Luo, W. P. Tay, and M. Leng, “Identifying infection sources and regions in large networks,” *IEEE Transactions on Signal Processing*, vol. 61, no. 11, pp. 2850–2865, 2013.
- [21] A. Sridhar and H. V. Poor, “Sequential estimation of network cascades,” in *Proceedings of the Asilomar Conference on Signals, Systems, and Computers*, 2020.
- [22] ———, “Bayes-optimal methods for finding the source of a cascade,” in *Proceedings of the IEEE International Conference on Acoustics, Speech, and Signal Processing*, 2021.
- [23] M. M. Bronstein, J. Bruna, Y. LeCun, A. Szlam, and P. Vandergheynst, “Geometric deep learning: going beyond euclidean data,” *IEEE Signal Processing Magazine*, vol. 34, no. 4, pp. 18–42, 2017.
- [24] Z. Wu, S. Pan, F. Chen, G. Long, C. Zhang, and S. Y. Philip, “A comprehensive survey on graph neural networks,” *IEEE Transactions on Neural Networks and Learning Systems*, vol. 32, no. 1, pp. 4–24, 2020.
- [25] F. Scarselli, M. Gori, A. C. Tsoi, M. Hagenbuchner, and G. Monfardini, “The graph neural network model,” *IEEE Transactions on Neural Networks*, vol. 20, no. 1, pp. 61–80, 2008.
- [26] C. Fan, L. Zeng, Y. Ding, M. Chen, Y. Sun, and Z. Liu, “Learning to identify high betweenness centrality nodes from scratch: A novel graph neural network approach,” in *Proceedings of the Conference on Information and Knowledge Management (CIKM)*, 2019.
- [27] V. La Gatta, V. Moscato, M. Postiglione, and G. Sperli, “An epidemiological neural network exploiting dynamic graph structured data applied to the COVID-19 outbreak,” *IEEE Transactions on Big Data*, vol. 7, no. 1, pp. 45–55, 2020.
- [28] C. Shah, N. Dehmamy, N. Perra, M. Chinazzi, A.-L. Barabási, A. Vespignani, and R. Yu, “Finding patient zero: Learning contagion source with graph neural networks,” *arXiv preprint arXiv:2006.11913*, 2020.
- [29] B. Awerbuch and R. Gallager, “A new distributed algorithm to find breadth first search trees,” *IEEE Transactions on Information Theory*, vol. 33, no. 3, pp. 315–322, 1987.
- [30] S. Even, *Graph Algorithms*. Cambridge University Press, 2011.
- [31] R. Graham, D. Knuth, and O. Patashnik, *Concrete Mathematics: a Foundation for Computer Science*. Addison-Wesley Professional, 1991.
- [32] T. N. Kipf and M. Welling, “Semi-supervised classification with graph convolutional networks,” in *Proceedings of the International Conference on Learning Representations (ICLR)*, 2016.
- [33] W. L. Hamilton, Z. Ying, and J. Leskovec, “Inductive representation learning on large graphs,” 2017.
- [34] Y. LeCun, Y. Bengio, and G. Hinton, “Deep learning,” *nature*, vol. 521, no. 7553, pp. 436–444, 2015.
- [35] K. Hornik, “Approximation capabilities of multilayer feedforward networks,” *Neural networks*, vol. 4, no. 2, pp. 251–257, 1991.
- [36] P.-D. Yu, C. W. Tan, and H.-L. Fu, “Rumor source detection in finite graphs with boundary effects by message-passing algorithms,” in *Proceedings of the 2017 IEEE/ACM International Conference on*

*Advances in Social Networks Analysis and Mining 2017*, ser. ASONAM '17. New York, NY, USA: ACM, 2017, pp. 86–90.

- [37] G. Chen, X. Wang, and X. Li, *Fundamentals of Complex Networks: Models, Structures and Dynamics*. John Wiley & Sons, 2014.
- [38] D. C. Adam, P. Wu, J. Y. Wong, E. H. Lau, T. K. Tsang, S. Cauchemez, G. M. Leung, and B. J. Cowling, “Clustering and superspreading potential of SARS-CoV-2 infections in Hong Kong,” *Nature Medicine*, vol. 26, no. 11, pp. 1714–1719, 2020.
- [39] B. Xu, M. U. Kraemer, and D. C. Group, “Open access epidemiological data from the COVID-19 outbreak,” *The Lancet. Infectious Diseases*, vol. 20, no. 5, p. 534, 2020.